Nuclear Engineering and Design 50 (1978) 379–385

ANALYTICAL DETERMINATION OF HEAT FLOW SHAPE FACTORS FOR COMPOSITE, PRISMATIC BARS OF DOUBLY-CONNECTED CROSS SECTION

P.A.A. LAURA
Institute of Applied Mechanics, 8111 Base Naval Puerto Belgrano, Argentina
and
G. SANCHEZ SARMIENTO
Centro Atómico Bariloche – CNEA, 8400 San Carlos de Bariloche, Argentina

Received 26 October 1977

Cylindrical or prismatic configurations are used in many engineering situations (nuclear, mechanical, etc.). Oddly-shaped, doubly-connected geometries are required in some applications, and generated in general computer-oriented solutions by the research engineer. The title problem is solved in the present paper using an approximate conformal mapping approach. It is shown that the calculated shape factors are in good agreement with those obtained using a finite element code.

1. Introduction

Cylindrical or prismatic elements of odd-shaped, doubly-connected cross sections are used in a multitude of engineering applications: a graphite brick of a gas-cooled nuclear reactor, solid propellant rocket motors, wavequides commonly used in microwave engineering, etc.

On the other hand, depending upon the particular type of application, the use of two or more different materials may prove useful.

Consider the configurations shown in figs. 1 and 2 (w-plane). A general, analytical approach which yields the shape factor S for these configurations seems out of the question. But it will be shown that under certain restrictions, the shape factor S can be

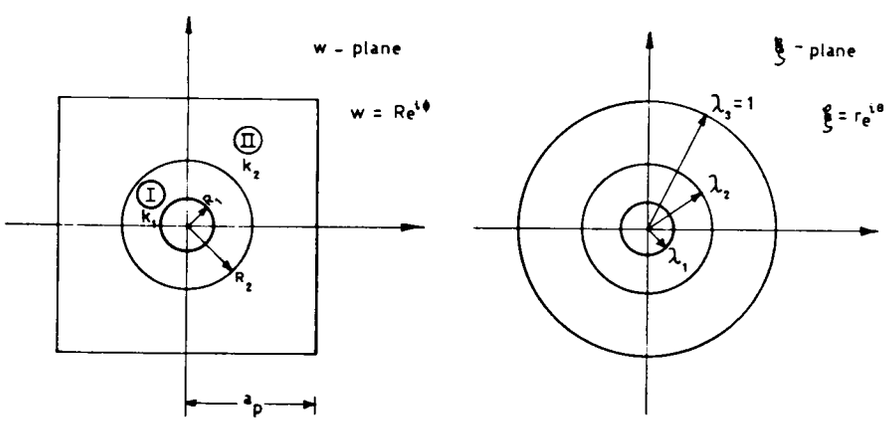

Fig. 1. Cross section of a prismatic, composite bar with a concentric circular perforation.

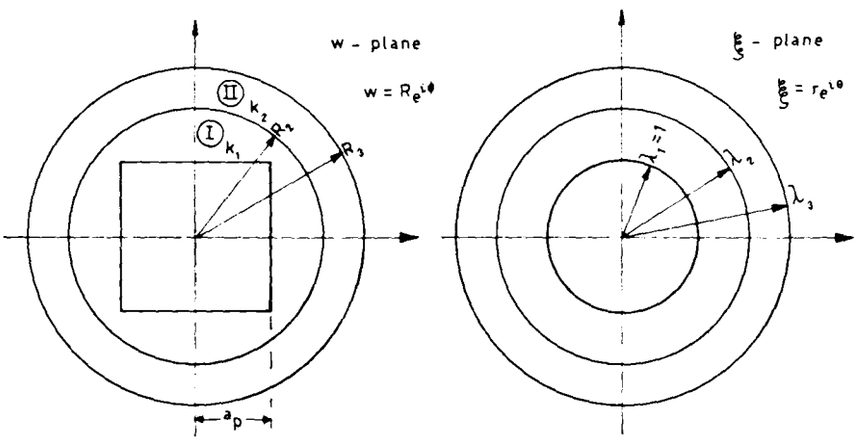

Fig. 2. Cross section of a circular, composite bar with a concentric perforation of regular polygonal shape.

obtained in a very simple fashion using an extermely simple approach.

2. An approximate conformal mapping method

Examine the composite, doubly-connected, annular configuration shown in fig. 3. One can easily show by standard techniques that the heat flow under steady state conditions between the inner surface ($r = a$) and the outer boundary ($r = c$) is given by the expression

$$q = Sk_1(T_1 - T_3)\,, \tag{1}$$

where

$$S = \frac{2\pi}{\ln(b/a) + ((k_1/k_2)\ln(c/b)}\,, \tag{2}$$

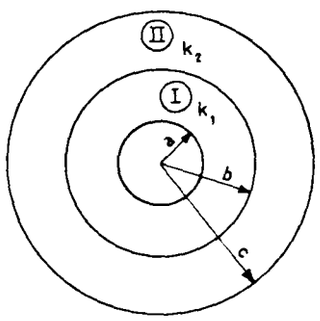

Fig. 3. Cross section of a composite, circular, annular bar.

T_1 = temperature maintained at $r = a$, and
T_3 = temperature maintained at $r = c$.

If the domains of the w-plane of figs. 1 and 2 were "mappable" onto the concentric annular domains shown in the same figures in the ξ-plane, one could use expression (2) replacing the radii a, b and c by the corresponding λ_1, λ_2 and λ_3. Clearly this is extremely difficult to achieve for any value of the ratios a_p/R_1 and R_2/R_1 (fig. 1) and R_3/a_p and R_3/R_2 in the case of the configuration in fig. 2.

However, an approximate mapping of the doubly-connected, composite domains can be obtained in a very simple fashion if

$$R_1, R_2 \ll a_p \quad \text{(fig. 1)}$$

and

$$R_2, R_3 \gg a_p \quad \text{(fig. 2)}\,.$$

This fact is a direct conclusion of the developments of refs. [1] and [2], where only a single material was assumed. A regular, simply-connected polygonal shape in the w-plane was mapped onto a unit circle in the ξ-plane by an infinite series of the form

$$w = a_p A_s \sum_{j=0}^{\infty} a_{1+sj}\,\xi^{1+sj}; \qquad a_1 = 1\,, \tag{3}$$

where A_s = coefficient (table 1), s = order of the polygon, and $\xi = re^{i\theta}$.

Take now circles defined by $r = \lambda_1, \lambda_2$ where $\lambda_1, \lambda_2 \ll 1$. Obviously only the first term of (3) will

Table 1
Values of A_s and A'_s as a function of the order of the polygon, s

s	A_s	A'_s
4	1.08	1.1812
5	1.0526	1.0993
6	1.0376	1.0632
7	1.0279	1.0438
8	1.0219	1.0323

predominate and the corresponding images in the w-plane will be approximate circles of radii

$$R_1 \simeq a_p A_s \lambda_1 , \tag{4a}$$

and

$$R_2 \simeq a_p A_s \lambda_2 . \tag{4b}$$

Making

$$(a, b, c) = (\lambda_1, \lambda_2, 1) , \tag{5}$$

one obtains, substituting eqs. (4) and (5) into eq. (2):

$$S = \frac{2\pi}{\ln \frac{R_2}{R_1} + \frac{k_1}{k_2} \ln \frac{a_p}{R_2} + \frac{k_1}{k_2} \ln A_s} \tag{6}$$

Making $k_1 = k_2$ and $R_1 = R_2$, eq. (6) degenerates into expression (14) of ref. [1]. Clearly the accuracy of (6) will deteriorate when R_1 and/or R_2 become rather large in comparison with the apothem of the polygon, a_p.

The approach is similar in the case of configurations such as those shown in fig. 2. One deals now with the function which transforms the infinite plane with a hole of regular polygonal shape (w-plane) onto the infinite plane with a circular perforation of unit radius (ξ-plane):

$$w = a_p A'_s \sum_{j=0}^{\infty} a_{1-sj} \xi^{1-sj} , \tag{7}$$

where A'_s = coefficient (see table 1).

Taking now $r >> 1$ the first term of (7) will predominate and the corresponding, approximate circles in the w-plane will be defined by their radii:

$$R_2 = a_p A'_s \lambda_2 , \tag{8a}$$

$$R_3 = a_p A'_s \lambda_3 . \tag{8b}$$

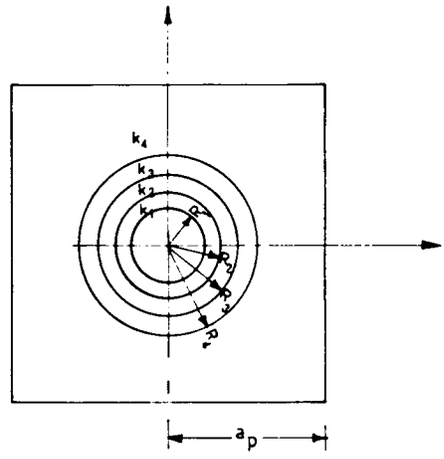

Fig. 4. Cross section of a prismatic, composite bar of four different materials with a concentric circular perforation.

Making

$$(a, b, c) = (1, \lambda_2, \lambda_3) , \tag{9}$$

and replacing (8) and (9) in eq. (2), one obtains:

$$S = \frac{2\pi}{\ln \frac{R_2}{a_p} - \ln A'_s + \frac{k_1}{k_2} \ln \frac{R_3}{R_2}} \tag{10}$$

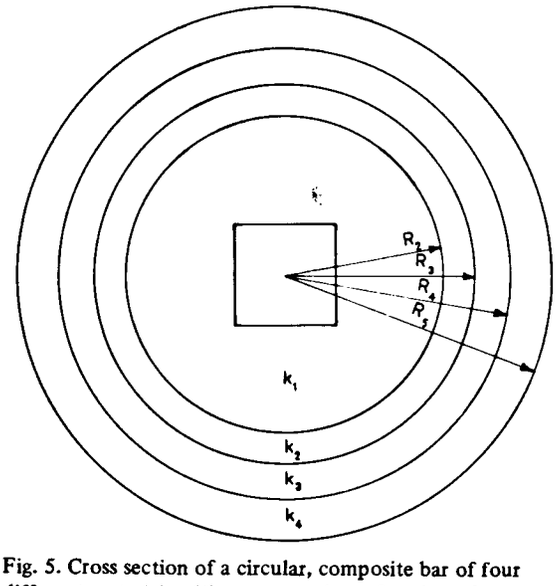

Fig. 5. Cross section of a circular, composite bar of four different materials with a concentric perforation of regular polygonal shape.

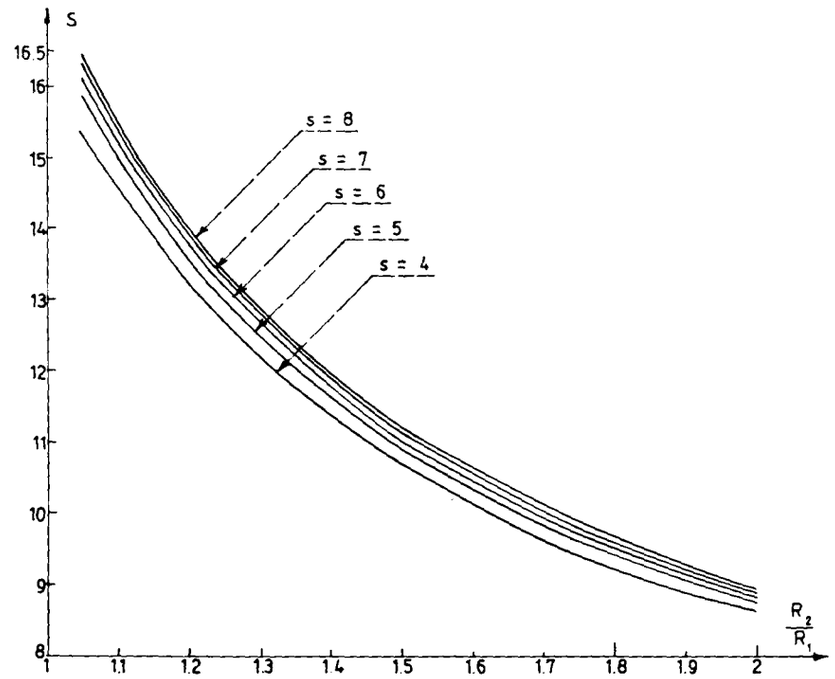

Fig. 6. Shape factor S as a function of R_2/R_1 and s for a regular polygonal shape with a concentric circular perforation k_2/k_1 = 2.0; a_p/R_1 = 2.0.

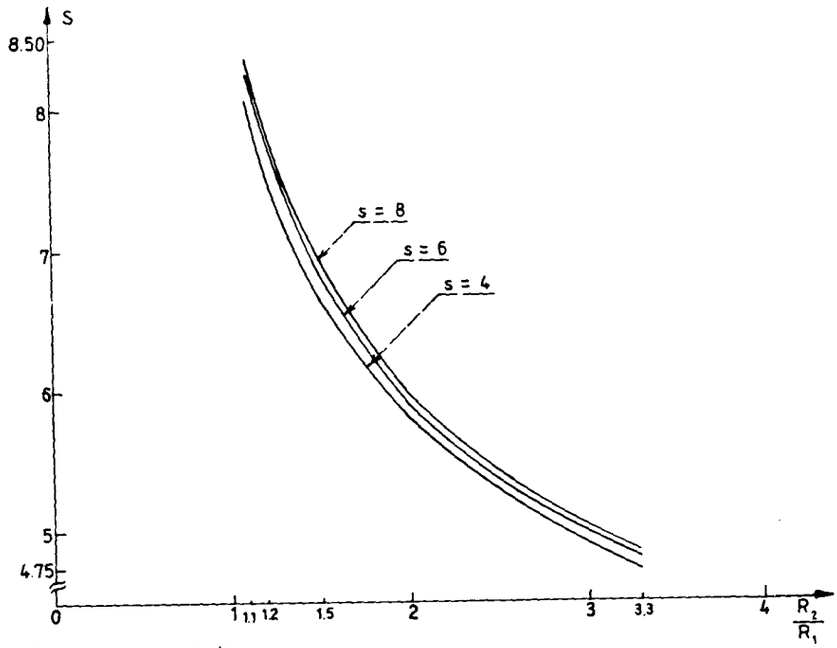

Fig. 7. Shape factor S as a function of R_2/R_1 and s for a regular polygonal shape with a concentric circular perforation k_2/k_1 = 2.0; a_p/R_1 = 4.0.

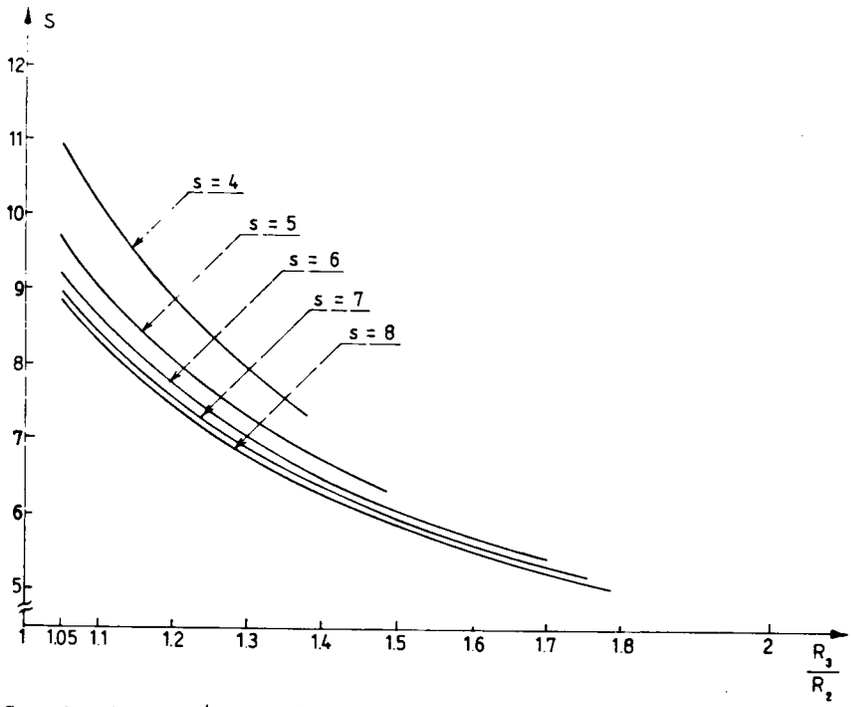

Fig. 8. Shape factor S as a function of R_3/R_2 and s for a circular outer boundary with a concentric perforation of regular polygonal shape $k_2/k_1 = 0.5$; $R_3/a_p = 2.0$.

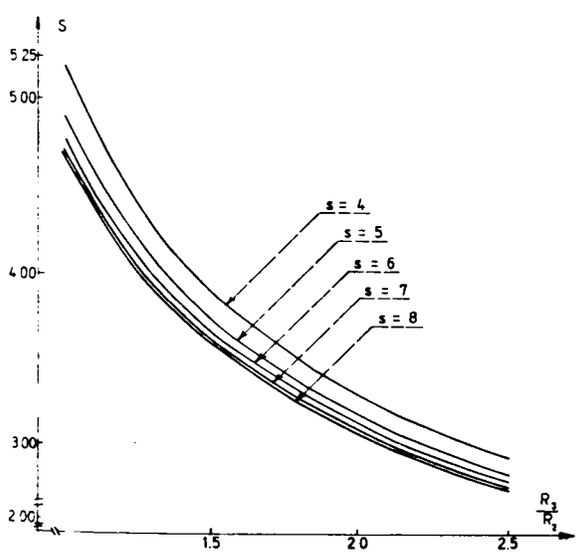

Fig. 9. Shape factor S as a function of R_3/R_2 and s for a circular outer coundary with a concentric perforation of regular polygonal shape. $k_2/k_1 = 0.5$; $R_3/a_p = 4.0$.

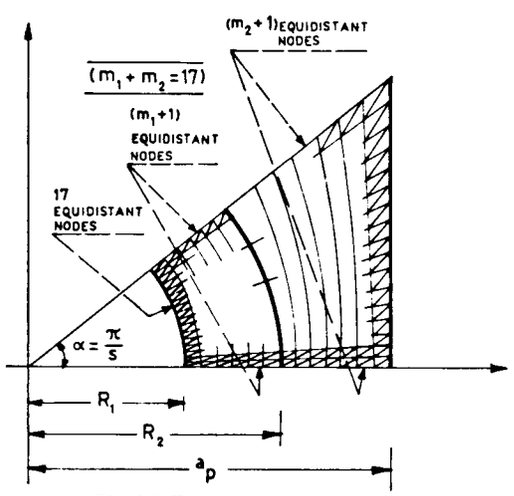

Fig. 10. Element distribution.

Table 2
Comparison of analytical and finit elements predictions (prismatic, composite bar of regular polygonal shape with a concentric circular perforation)

R_2/R_1	a_p/R_1	s	m_1	m_2	S	
					Finite elements	Conformal mapping
1.10	2.0	4	2	14	14.40	14.52
1.50	2.0	4	8	8	10.58	10.69
1.90	2.0	4	14	2	8.80	8.90
1.10	2.0	8	2	14	15.31	15.51
1.50	2.0	8	8	8	11.11	11.22
1.90	2.0	8	14	2	9.18	9.26
1.30	4.0	4	2	14	7.10	7.28
2.50	4.0	4	8	8	5.14	5.28
3.70	4.0	4	14	2	4.41	4.53
1.30	4.0	8	2	14	7.38	7.52
2.50	4.0	8	8	8	5.20	5.41
3.70	4.0	8	14	2	4.45	4.63

Making $k_1 = k_2$ and $R_3 = R_2$, expression (10) yields

$$S = \frac{2\pi}{\ln(R_3/a_p) - \ln A_s'}, \tag{11}$$

which agrees with the expression obtained in [2].

Obviously the accuracy of (10) improves as R_2 and R_3 increase in relation to a_p.

It is interesting to point out that the approach developed in this study is also applicable if more than two materials are used (figs. 4 and 5). Obviously, the same geometric restrictions are applicable.

Figs. 6–9 depict the variation of the shape factor S as a function of some of the geometric parameters involved.

3. Solution by means of the finite element method

Figs. 10 and 11 show the element distribution used in the present analysis. A comparison of values of shape factors between results obtained by means

Table 3
Comparison of analytical and finite elements predictions (cylindrical, composite bar with a concentric perforation of regular polygonal shape)

R_3/a_p	R_3/R_2	s	m_1	m_2	S	
					Finite elements	Conformal mapping
2.0	1.05	4	14	2	10.95	10.92
2.0	1.20	4	8	8	8.85	8.86
2.0	1.35	4	2	14	7.53	7.60
2.0	1.10	8	14	2	8.41	8.30
2.0	1.45	8	8	8	6.13	6.08
2.0	1.70	8	2	14	5.29	5.27
4.0	1.10	4	14	2	4.86	4.78
4.0	1.90	4	8	8	3.42	3.37
4.0	2.70	4	2	14	2.85	2.84
4.0	1.10	8	14	2	4.42	4.33
4.0	2.30	8	8	8	2.94	2.87
4.0	3.50	8	2	14	2.45	2.41

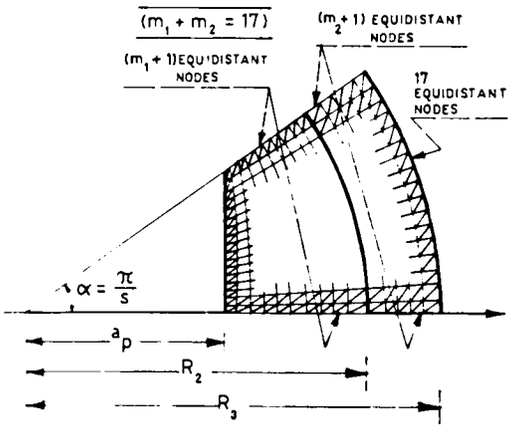

Fig. 11. Element distribution.

of expressions (6) and (10) and numerical results obtained by means of a finite element code are depicted in tables 2 and 3 (the parameter k_2/k_1 has been taken as 2 for the configuration in fig. 1 and as $\frac{1}{2}$ for fig. 2).

Agreement is excellent in all cases at least from an engineering viewpoint (even in those instances when the geometric restrictions assumed in deriving eqs. (6) and (10) are not satisfied, the analytical predictions agree well with the finite elements results).

References

[1] P.A.A. Laura and E. Susemihl, Nucl. Eng. Des. 25 (1973) 409.

[2] P.A.A. Laura and G. Sánchez Sarmiento, Nucl. Eng. Des. (to be published).